Journal of Solid State Chemistry **167,** 472–479 (2002)
doi:10.1006/jssc.2002.9664

Thermoelectric Properties (Resistivity and Thermopower) in ($Bi_{1.5}Pb_{0.5}Ca_{2-x}M_xCo_2O_{8-\delta}$ ($M = Sc^{3+}$, Y^{3+}, or La^{3+})

E. Iguchi,[1] S. Katoh, H. Nakatsugawa, and F. Munakata

Division of Materials Science and Engineering, Graduate School of Engineering, Yokohama National University, Tokiwadai, Hodogaya-Ku, Yokohama 240-8501, Japan

Received January 14, 2002; in revised form March 22, 2002; accepted May 28, 2002

In order to understand the origin of good thermoelectric (TE) properties in the transition metal oxides with the lattice structure isomorphous to the 232-structure, the bond nature between Co and O ions in $Bi_{1.5}Pb_{0.5}Ca_{2-x}M_xCo_2O_{8-\delta}$-system has been tried to vary by replacing M with Sc^{3+}, Y^{3+} or La^{3+} and by changing x from 0 to 0.3. The resistivity is minimum at $x = 0.1$ in Sc- and Y-systems, but very high in La-system. The large thermopower is obtained in every compound. The experimental TE properties have been discussed mainly within the framework of the charge-transfer scheme in which the ionic radii of Sc^{3+} and Y^{3+} smaller than Ca^{2+} reduce the energy between O 2*p* levels and Co e_g parentages but the large ionic radius of La^{3+} expands it. The oxygen solubility in the compounds and the lattice distortion peculiar to the 232-structure are also likely to contribute somewhat to the experimental results.

Key Words: **thermoelectric material; transition metal oxides; 232-lattice structure; thermoelectric properties; electrical transport properties; resistivity; thermopower; magnetic properties; charge transfer; two band model.**

1. INTRODUCTION

Thermoelectric (TE) materials have recently attracted a renewed interest as an application to a clean energy-conversion system that utilizes the waste heat of high temperature (1). The conversion efficiency of a TE material is characterized by the TE figure of merit $Z = S^2/\rho\kappa$, where S, ρ and κ are thermopower (Seebeck's coefficient), resistivity and thermal conductivity. A good TE material involves then high thermopower and low resistivity with low thermal conductivity. A high magnitude for Z is however difficult to realize because these parameters do not change independently. In most materials where band conduction dominates electronic transports like degenerated semiconductors and intermetallic compounds, a high concentration of carriers responsible for low resistivity generally results in high thermal conductivity (2). Owing to this reason, the utilization of the conventional TE materials is unfortunately restricted within narrow limits. They are used either at rather low temperature or in vacuum because they contain serious problems of oxidation, decomposition and melting at high temperature in air. TE materials applicable to a clean energy-conversion system require a function to overcome these problems.

From this view, metal oxides are of great advantage to material syntheses and also to a long-term use at high temperature in air. The development of new metal oxides with high Z is then of great importance. The layered perovskite cobalt oxides such as $(Na,Ca)Co_2O_4$ (3, 4) and $Ca_3Co_4O_9$ (5) are promising candidates for high temperature-TE materials. The recent study on $(Na,Ca)Co_2O_4$ indicates the importance of a misfit structure resulting from bidimensional matching of two different structures, such as rock-salt-typed layers and CdI_2-type layers, in TE properties (6). $Bi_{2-x}Pb_xSr_{3-y}Y_yCo_2O_{9-\delta}$ also involves high potential for a high TE figure of merit Z, as our previous report indicates (7). Since our previous study on $Bi_{2-x}Pb_xSr_{3-y}Y_yCo_2O_{9-\delta}$ mostly concentrated only on developing of a high temperature material with a high TE figure of merit (7), an elucidation to clarify the reasons for the concomitant emergence of low resistivity and high thermopower is now required.

Abbate *et al.* (8, 9) point out the importance of the charge-transfer (CT) scheme so as to understand electrical transport properties in Co-oxides of the strongly correlated electron system. This suggests that the Co–O network plays an important role in TE properties and must be mainly responsible for low resistivity and high thermopower. If layer structures of upper and lower sides of the Co–O

[1] To whom correspondence should be addressed. Department of Mechanical Engineering and Matericals Science, Faculty of Engineering, Yokahama National University, Tokiwadai, Hodogaya-ku, Yokohama 240-8501, Japan. Fax: +81-45-331-6593. E-mail: iguchi@post.me.ynu.ac.jp

0022-4596/02 $35.00

networks in a crystal lattice are modulated artificially so that a smooth variation in the bond nature between Co and O ions may take place in progression, then, it would be possible to obtain significant knowledge as to the emergence of low resistivity and high thermopower.

Based upon the strategy like this, the present study has prepared the compounds in $Bi_{1.5}Pb_{0.5}Ca_{2-x}M_xCo_2O_{8-\delta}$-system by replacing M with Sc^{3+}, Y^{3+} or La^{3+}, and also by employing $x = 0$, 0.1, 0.2 and 0.3. Sc^{3+}, Y^{3+} and La^{3+} have the similar electronic structures, i.e., ns^2np^6, and the ionic radius increases progressively with increasing n from 3 (Sc^{3+}) to 5 (La^{3+}) (10). Instead of $Bi_{1.5}Pb_{0.5}Sr_{2-x}M_xCo_2O_{8-\delta}$-system, $Bi_{1.5}Pb_{0.5}Ca_{2-x}M_xCo_2O_{8-\delta}$-system has been employed because the ionic radius of Ca^{2+} is larger than those of Sc^{3+} and Y^{3+} and smaller than that of La^{3+} whereas Sr^{2+} has the ionic radius larger than the radii of all of these trivalent ions (10). These procedures are expected to enable a smooth variation in the nature of the Co–O bonds in the networks. In comparison with $(Bi,Pb)_2(Ca,M)_3Co_2O_{8-\delta}$ system, there must be other appropriate oxide-systems which include the significant knowledge on the correlation between Co–O networks and good TE properties. The present study has carried out, however, the TE experiments on $Bi_{1.5}Pb_{0.5}Ca_{2-x}M_xCo_2O_{8-\delta}$-system because we want to understand the emergence-kinetic of the good TE properties in $Bi_{2-x}Pb_xSr_{3-y}Y_yCo_2O_{9-\delta}$ investigated in our previous report (7).

The present study has investigated TE properties of $Bi_{1.5}Pb_{0.5}Ca_{2-x}M_xCo_2O_{8-\delta}$, not $Bi_{1.5}Pb_{0.5}Ca_{3-x}M_xCo_2O_{9-\delta}$, because of the following reasons. Polycrystalline $Bi_2Ca_3Co_2O_{9-\delta}$ ceramics contain often unexpected impurity phases (11). In fact, $Bi_{2-x}Pb_xSr_{3-y}Y_yCo_2O_{9-\delta}$ with the structure nearly isomorphous to $Bi_2Ca_3Co_2O_{9-\delta}$ is not a single phase and impurity phases like $Bi_2Sr_2O_5$ and $SrCoO_y$ segregate along boundaries (12). The volume fractions of these impurity phases are never negligibly small and moreover, these phases interfere with the elucidation of TE properties of the bulks in the ceramics specimen very seriously as described in our previous report (7). Ceramic compounds of a single phase are, however, rather easy to produce in $(Bi,Pb)_2Sr_2Co_2O_{8-\delta}$-system (6, 13). Furthermore, even in $Bi_2Sr_{2-x}M_xCo_2O_{8-\delta}$, the main XRD pattern corresponds very well to that of $Bi_2Sr_3Co_2O_{9-\delta}$ (the 232-typed lattice) (12, 14, 15), although the XRD pattern includes very weak satellite lines due to impurity phases. Therefore, TE properties obtained experimentally in $Bi_{1.5}Pb_{0.5}Ca_{2-x}M_xCo_2O_{8-\delta}$-system are expected to result mainly from $Bi_{1.5}Pb_{0.5}Ca_{3-x}M_xCo_2O_{9-\delta}$.

Referring to these arguments, the measurements of TE properties (resistivity and thermopower) on $Bi_{1.5}Pb_{0.5}Ca_{2-x}M_xCo_2O_{8-\delta}$-system have been carried out with the magnetic measurements. Some knowledge on Co spin states available from the magnetic measurements would be important even if the oxygen deficiency in the compounds bring about mixed valence states of Co ions.

2. EXPERIMENTAL DETAILS

$Bi_{1.5}Pb_{0.5}Ca_{2-x}M_xCo_2O_{8-\delta}$ polycrystalline ceramics specimens ($M = Sc^{3+}$, Y^{3+} or La^{3+}) were prepared by the conventional solid-state synthesis technique. Bi_2O_3, PbO_2, $CaCO_3$, Y_2O_3, Sr_2O_3, La_2O_3, and Co_3O_4 powders were used. The present study changes x from 0 to 0.3 for $M = Sc^{3+}$ and Y^{3+}. In the case of $M = La^{3+}$, $x = 0.2$ is employed. First, mixed powders were calcined in air at 770–790°C for 12 h in air. The heating temperature depends on the ionic species of the substitute for Ca^{2+} ions and their amounts, i.e., x. After being ground very carefully and mixed well, powders were pressed into pellets and sintered finally in air at 830–850°C for 12–18 h.

After investigating lattice structures using Cu $K\alpha$ X-ray diffraction (XRD), four-probe dc resistivity and thermopower (Seebeck's coefficient) below room temperature have been measured as a function of temperature in the following way. A Keithley 619 resistance bridge, an Advantest TR 6871 digital multimeter and an Advantest R 6161 power supply were used for dc-resistivity measurements. Thermopower measurement was carried out on a sample placed between two blocks of oxygen-free high conductivity (OFHC) copper. Both ends of the sample were coated with silver paste and then placed in contact with thin copper plates. Copper–constantan thermocouples were welded to the reverse sides of the copper plates to measure temperature and thermopower. The temperature difference between both ends of a specimen is 10–15 K. The magnetic susceptibilities, χ, were measured with the magnetic field of 1 kOe by a SQUID (Quantum Design MPMS) in the temperature range up to 300 K. The copper–constantan pre-calibrated at 4.2, 77 and 273 K was used for the temperature measurements.

3. EXPERIMENTAL RESULT

The main XRD pattern of $Bi_{1.5}Pb_{0.5}Ca_{2-x}M_xCo_2O_{8-\delta}$ prepared in the present study agrees with that in $Bi_2Ca_3Co_2O_9$ reported by Vashuk *et al.* (11) and Tarascon *et al.* (14). Figure 1 demonstrates one example, i.e., the XRD pattern for $Bi_{1.5}Pb_{0.5}Ca_{1.7}Y_{0.3}Co_2O_{8-\delta}$ ($x = 0.3$ and $M = Y^{3+}$), and the XRD pattern of $Bi_2Ca_3Co_2O_9$ (the 232-typed structure) is also attached for reference (11). Despite $Bi_{1.5}Pb_{0.5}Ca_{2-x}M_xCo_2O_{8-\delta}$, the main XRD pattern is nearly the same as that of the 232-structure. Since satellite lines due to impurity phases are difficult to detect in Fig. 1 compared with the $Bi_{2-x}Pb_xSr_{3-y}Y_yCo_2O_{9-\delta}$-system (7), the XRD patterns in the present study give an indication of small volume fractions of impurity phases even if they

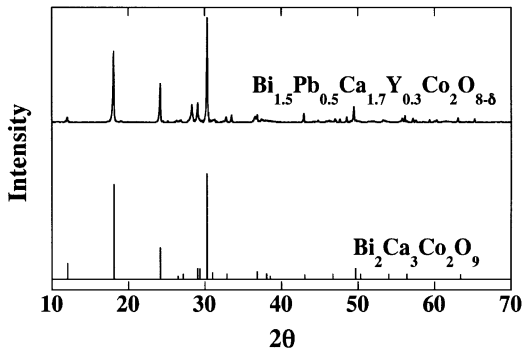

FIG. 1. X-ray diffraction (XRD) pattern of $Bi_{1.5}Pb_{0.5}Ca_{1.7}Y_{0.3}Co_2O_{8-\delta}$ with XRD of $Bi_2Ca_3Co_2O_9$ with the 232-structure.

coexist with the main phase of the 232-typed structure. The lattice parameter c is estimated by the least-squares methods, using (00l) family. In every specimen except the La-system ($M = La^{3+}$), the lattice parameter c decreases linearly with x. When $x = 0$, c is 29.497 Å but it decreases to 29.439 Å at $x = 0.3$ for the Sc-system ($M = Sc^{3+}$) and to 29.398 Å at $x = 0.3$ for the Y-system ($M = Y^{3+}$). In the La-system, $c = 29.565$ Å at $x = 0.2$.

Figures 2(a)–2(c) depict the relations of the four-probe dc resistivity ρ and temperature T as a parametric function of x in $Bi_{1.5}Pb_{0.5}Ca_{2-x}M_xCo_2O_{8-\delta}$. It is noteworthy that both of the Sc- and Y-systems have the common feature, i.e., the minimum resistivity at $x = 0.1$ and an increase in ρ with x increasing from 0.1 to 0.3. The minimum resistivity in the both systems is about 0.1 Ω cm which is however large approximately by one order, in comparison with the minimum resistivity in the $Bi_{2-x}Pb_xSr_{3-y}Y_yCo_2O_{9-\delta}$ system ($x = y = 0.5$) (7). The La-system ($x = 0.2$) involves the high resistivity, which is larger than the resistivity of the Sc- and Y-systems ($x = 0.2$) by more than one order. Every specimen exhibits the semiconductive electrical transport

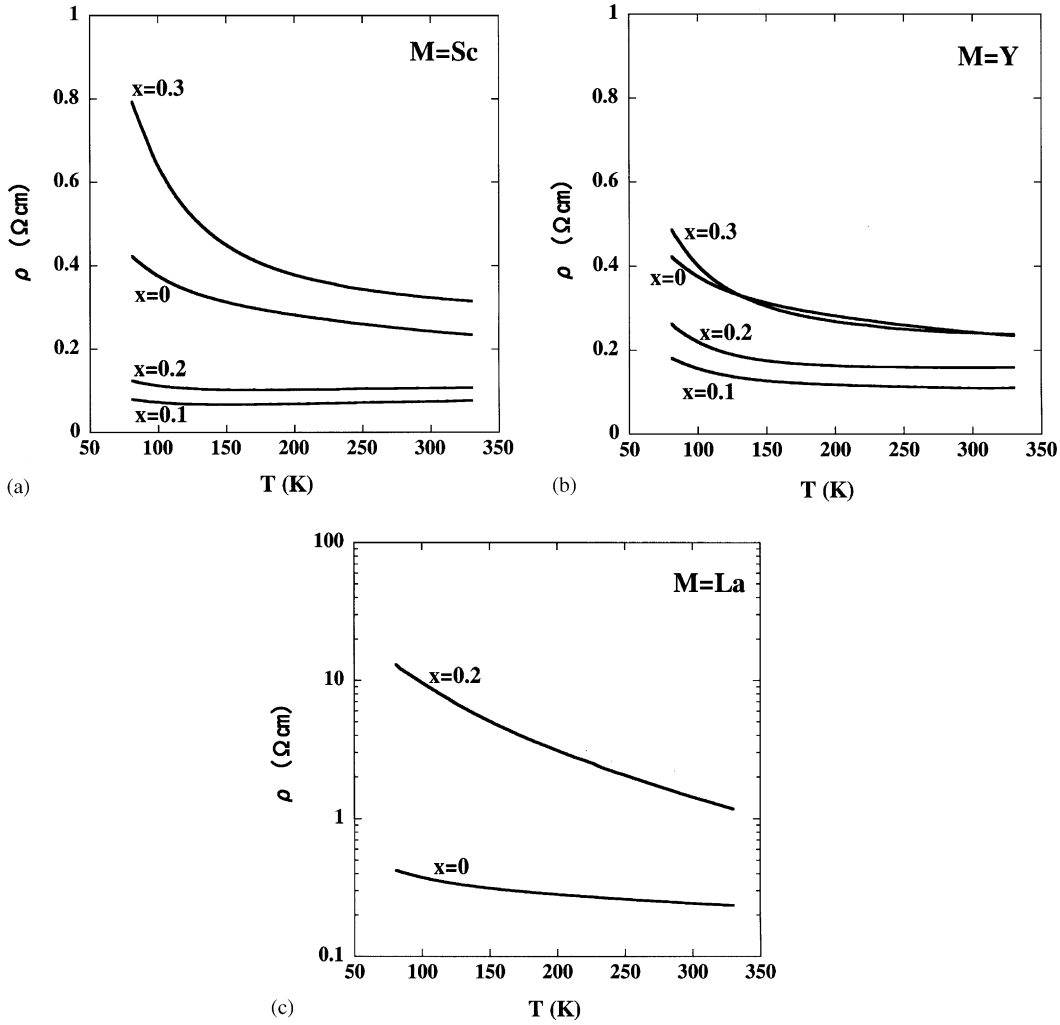

FIG. 2. Four-probe dc resistivity ρ against T as a parametric function of x for $Bi_{1.5}Pb_{0.5}Ca_{2-x}M_xCo_2O_{8-\delta}$ where $M = Sc^{3+}$ (a), Y^{3+} (b) and La^{3+} (c).

except the $x = 0.1$ and 0.2 compounds in the Sc-system and the $x = 0.1$ compound in the Y-system, which show the metallic behavior.

Figure 3 plots thermopower S against T for the $x = 0.2$ compound in each system with the $x = 0$ compound. The magnitudes for S in the present series are nearly in the same order as the thermopower in the $Bi_{2-x}Pb_xSr_{3-y}Y_yCo_2O_{9-\delta}$-system (7). As well as the resistivity, the La-doped compound shows the peculiar thermopower-behavior, i.e., the steep drop with T decreasing from 160 K.

Figure 4a and 4b demonstrate temperature dependencies of the inverse molar magnetic susceptibility χ^{-1} for the Sc- and Y-systems. In these systems, the Curie–Weiss law holds, i.e., $\chi = C/(T - \Theta)$, where C is the Curie constant and Θ the Weiss temperature. Such magnetic behavior is very different from that of the $Bi_{2-x}Pb_xSr_{3-y}Y_yCo_2O_{9-\delta}$-system (7). This must imply the nearly single phase in every compound of the Sc- and Y-systems because the $Bi_{2-x}Pb_xSr_{3-y}Y_yCo_2O_{9-\delta}$-system exhibits the very complicated magnetic behavior due to the impurity phases such as $Bi_2Sr_2O_5$ and $SrCoO_y$ (7). In both of Sc- and Y-systems, χ^{-1} is maximum at $x = 0.1$ and decreases when x increases from 0.1 to 0.3. Using the theoretical relation of $\mu_{\text{eff}} \cong \sqrt{8C}\,\mu_B$ (16), the experimental values for the Curie constant C obtained by the least-squares methods yield $\mu_{\text{eff}} = 1.29\,\mu_B$ at $x = 0$, $1.14\,\mu_B$ at $x = 0.1$, $1.44\,\mu_B$ at $x = 0.2$ and $1.67\,\mu_B$ at $x = 0.3$ for the Sc-system, while $1.27\,\mu_B$ at $x = 0.1$, $1.43\,\mu_B$ at $x = 0.2$ and $1.46\,\mu_B$ at $x = 0.3$ for the Y-system, where μ_B is the Bohr magneton. It is interesting that ρ and μ_{eff} are minimum at $x = 0.1$ in both of the Sc- and Y-systems. As well as other 232-typed lattice such as $Bi_2Sr_3Co_2O_{9-\delta}$ (15), μ_{eff} in the present systems are larger in values than the expected ones. The mixed valences of Co ions due to the oxygen deficiency must be one of the reasons for the high effective magnetic moment.

Figure 4c shows the temperature dependencies of susceptibility (χ) in field cooling run (FC) at $H = 1$ kOe and field warming run after zero-field-cooled (ZFC) for the La-compound ($x = 0.2$). At $T > 200$ K, the FC curve and the ZFC curve are in agreement and the Curie–Weiss law also holds with $\mu_{\text{eff}} = 1.89\,\mu_B$. At $T < 160$ K, however, the ZFC curve has a maximum around 50 K whereas the FC curve exhibits the monotonous increase with T decreasing. Such magnetic behavior at low temperature is similar to that of Pb-doped Bi-Sr-Co–O misfit layer compound that involves antiferromagnetic interactions (17).

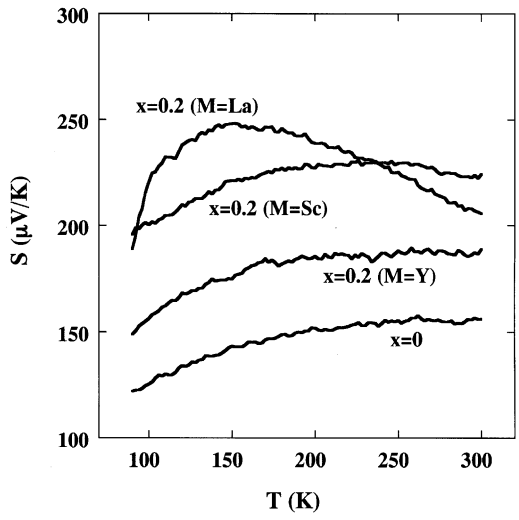

FIG. 3. S vs T for $Bi_{1.5}Pb_{0.5}Ca_2Co_2O_{8-\delta}(x = 0)$ and $Bi_{1.5}Pb_{0.5}Ca_{1.8}M_{0.2}Co_2O_{8-\delta}(x = 0.2)$ where $M = Sc^{3+}$, Y^{3+} and La^{3+}.

4. DISCUSSION

4.1. Lattice Structure

Despite $Bi_{1.5}Pb_{0.5}Ca_{2-x}M_xCo_2O_{8-\delta}$, the main XRD pattern in every compound agrees with that of the $Bi_2M_3Co_2O_9$ (232-type) structure as shown in Fig. 1 (11, 14, 15). In XRD pattern in each specimen, there are also satellite peaks due to impurity phases but they are very weak in comparison with $Bi_{2-x}Pb_xSr_{3-y}Y_yCo_2O_{9-\delta}$ (7). These results coincide with the description in the Introduction. According to the nominal compositions, Co-impurity phases and Bi-impurity phases must be involved in these compounds, but their contributions to the electronic and magnetic properties must be not so serious as $Bi_{2-x}Pb_xSr_{3-y}Y_yCo_2O_{9-\delta}$ because their volume fractions are presumed very slight as the XRD results show. Then the electronic and magnetic properties in $Bi_{1.5}Pb_{0.5}Ca_{2-x}M_xCo_2O_{8-\delta}$-system are mainly ascribed to the 232-typed crystal lattice.

4.2. Resistivity in Sc- and Y-systems

It is interesting to investigate whether there is some correlation between the (CT) and the electronic transport properties in the present systems as well as other 232-typed compounds investigated previously (14, 18–22). If the CT scheme is realized, the relative positions of the energy levels in $Bi_{1.5}Pb_{0.5}Ca_2Co_2O_{8-\delta}$ ($x = 0$) are; Co $3d$ t_{2g} < O $2p \leq$ Co $3d$ e_g. It is noteworthy that the oxygen deficiency must result in some amount of e_g electrons even at $x = 0$.

When Sc or Y ions are doped, the lattice constant along the c-axis decreases gradually with the amount of the doped ions, owing to the ionic radii of Sc^{3+} and Y^{3+} smaller than Ca^{2+} (10). The decrease in the lattice parameter c leads to the reduction of the ionic spaces between Co and O ions. The theoretical calculation predicts the shrinkage of the CT energy gaps between O $2p$ and Co e_g levels by the reduction in Co–O spaces (23). This prediction is also supported by the metal-insulator

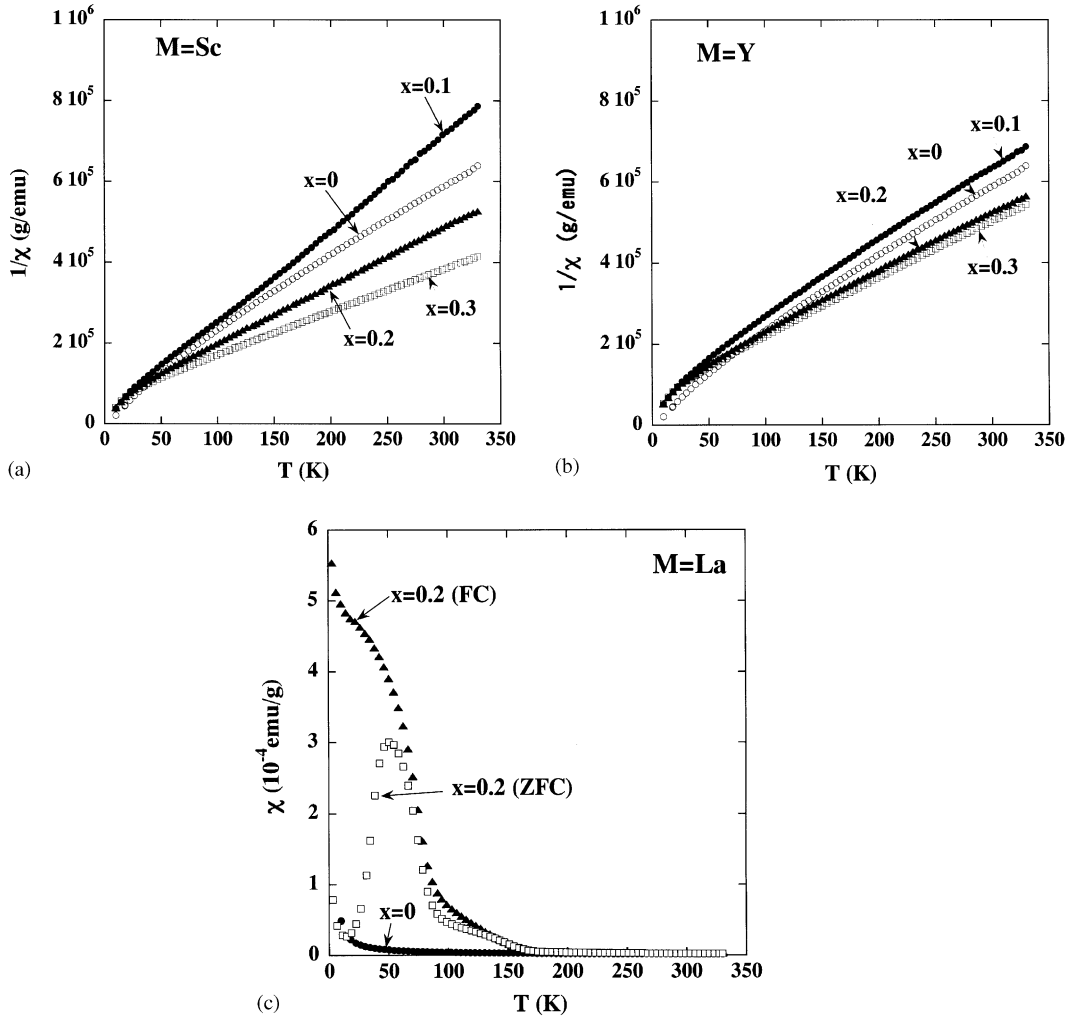

FIG. 4. Relations of χ^{-1} and T as a parametric function of x for $M = Sc^{3+}$ (a) and Y^{3+} (b), and relations of χ and T for the La-doped compound ($x = 0.2$) in field cooling (FC) run at $H = 1$ kOe and in the warming run after zero filed cooling (ZFC) with the result of the $x = 0$ compound (c).

(MI) transition in $LaCoO_3$ by the decrease in the ionic spaces between Co^{3+} and O^{2-} ions at high temperature (23, 24).

In each of Sc- and Y-systems, the resistivity is minimum at $x = 0.1$, but it increases with x increasing from 0.1 as shown in Fig. 2. Though the reason responsible for this result is still unknown, there are three possibilities to consider. Sc- or Y-doping has two functions; one is to reduce the Co–O ionic spaces as described just above and another one is electron-doping. The first possibility is that the reduction effect of the Co–O spacing may be stronger than the electron-doping effect at $x = 0.1$ but the latter effect may exceed the former one at high x. This is not inconsistent with the CT scheme as described below.

When the CT gaps shrink, the electron excitation from O $2p$ to Co e_g levels is enhanced. Then the hole-density in O $2p$ levels increases whereas Co e_g parentages contain the electrons excited from O $2p$ levels besides the electrons due to the oxygen deficiency. Since the O $2p$ holes are itinerant and have high mobility compared with the $3d$ electrons which are rather localized even in Co e_g levels, the O $2p$ holes predominantly dominate the electronic transport properties in Sc- or Y-doped compounds as the positive thermopower in Fig. 3 shows. When x is high, the density of the O $2p$ holes must decrease because the electrons doped by Sc- or Y-substitution occupy preferentially O $2p$ levels and compensate O $2p$ holes, and, as a result, the resistivity increases. The CT scenario then seems possible to describe the resistivity behaviors in the present systems. This must imply that the number of oxygen vacancies is not so large as the number that changes the main electronic conduction from the CT scheme to others, although the oxygen deficiency may bring about various Co states with different coordination.

The second possibility is the effect of oxygen content in the compounds. If a Sc- or Y-doped compound of $x = 0.1$

could accommodate oxygen ions the amount of which is larger than the oxygen content at $x = 0$, then the minimum resistivity in the compounds of $x = 0.1$ would be possible because the excess oxygen ions have the hole-doping effect, increasing the density of the O 2*p* holes. The last possibility is the lattice distortion. On the analogy of other 232-typed oxides (25), there must be also some lattice distortion in the $Bi_{1.5}Pb_{0.5}Ca_{2-x}M_xCo_2O_{8-\delta}$ compounds. If the lattice distortion is minimum at $x = 0.1$, the mean free path of the itinerant O 2*p* holes would become large and then the high mobility would yield the minimum resistivity at $x = 0.1$.

As shown in Fig. 2a and 2b, Sc-doped compounds ($x = 0.1$ and 0.2) and the Y-doped compound ($x = 0.1$) have low resistivity. As temperature increases, the resistivity in these compounds decreases like others but increases slightly with a further increase of temperature. Then a weak MI transition occurs in these specimens. In the high temperature range in which the metallic conduction takes place, the orbits of the O 2*p* holes and the 3*d* e_g electrons are extended thermally and then both of O 2*p* and Co e_g bands energetically somewhat broaden. Since the CT gaps shrink by Sc- or Y-doping, there is a high possibility that a partial overlap of O 2*p* levels and Co e_g parentages takes place. This must be the main reason for the weak MI transition observed in these compounds.

4.3. Magnetic Behaviors in Sc- and Y-Systems

The magnetic measurements on the present systems provide the only indirect knowledge on Co valence states because of the oxygen deficiency as described before. However, some speculation over the general outline of the magnetic structures would be possible even if the results in Fig. 4a and 4b are employed. If the electrons doped by Sc- or Y-substitution occupy Co e_g levels preferentially, the effective magnetic moment μ_{eff} would increase in proportion to the amount of Sc or Y ions. In the experiments on both the systems, however, the effective magnetic moments relatively decrease when x increases from 0 to 0.1. Furthermore, the resistivity is also minimum at $x = 0.1$ in each system as described before. In order to account for these facts, the CT scheme is likely to need some contribution from the effect of oxygen content. The oxygen contents in the specimens of $x = 0.1$ must be larger than that at $x = 0$ as described before and the hole-doping effect due to the oxygen increases the density of O 2*p* holes whereas some excess O 2*p* holes are compensated by e_g electrons based upon the requirement of the thermal equilibrium.

At $x \geq 0.2$, the increase in the amount of the electrons in O 2*p* levels due to Sc- or Y-doping decreases the concentration of the O 2*p* holes and increases the number of the electrons excited to Co e_g. Then both of ρ and μ_{eff} increase with x increasing from 0.1.

4.4. Two-band model

The arguments described above indicate that the Sc- or Y-doped compounds contain not only the itinerant O 2*p* holes but also the 3*d* e_g electrons. The electronic and thermopower properties in the present systems are then described by the two-band model, i.e., O 2*p* holes and 3*d* e_g electrons (26–28). The following formulae hold in the two-band model, $1/\rho = 1/\rho_1 + 1/\rho_2$ and $S = (\rho/\rho_1)S_1 + (\rho/\rho_2)S_2$ (29, 30). The first formula implies that both of O 2*p* holes and 3*d* e_g electrons formally contribute to the electrical transport properties. However, the effective contribution results mainly from the O 2*p* holes because of the low mobility of 3*d* e_g electrons compared with the high mobility of O 2*p* holes. Though both of O 2*p* holes and e_g electrons also contribute to the thermopower as the second formula indicates, e_g electrons yield negative thermopower whereas O 2*p* holes positive thermopower. Then the contribution of e_g electrons to the thermopower has a more direct effect than the contribution to the resistivity. In such a meaning, the thermopower due to the localized 3*d* e_g electrons cannot be neglected experimentally. In Sc- or Y-doped compounds, however, the positive thermopower in Fig. 3 indicate that O 2*p* holes dominate predominantly not only the electronic conduction but also the thermopower.

4.5. La-Doped Compound ($x = 0.2$)

The resistivity of the La-doped compound ($x = 0.2$) is larger than that of Sc- or Y-doped one ($x = 0.2$) by more than one order as shown in Fig. 2. The effective magnetic moment at $T > 200$ K is also considerably large, $\mu_{eff} = 1.89\,\mu_B$. Since the ionic radius of La^{3+} larger than Ca^{2+} expands the CT gaps through the enlargement in Co–O spaces (10, 23), the electron excitation from O 2*p* to Co e_g levels becomes less active and accordingly the concentrations of O 2*p* holes and 3*d* e_g electrons excited from O 2*p* levels are small in comparison with those in Sc- or Y-doped compounds. Consequently, the electrons doped by La-substitution cannot help occupying Co e_g parentages because the amount of the electrons which O 2*p* levels with small hole-densities can accommodate is less than that of O 2*p* levels in Sc- or Y-doped compounds. The high resistivity due to the decrease in the densities of mobile carriers and a large effective magnetic moment due to the increase in the number of 3*d* e_g electrons are then expected in the La-doped compound. The experimental results show that these are actually realized.

The contribution of 3*d* e_g electrons to the thermopower is recognized clearly in the La-doped compound ($x = 0.2$). Since the resistivity in this compound is very high, large thermopower is also expected. Experimentally, however, the thermopower of the La-doped specimen is in the same

order as that of Sc- or Y-doped compounds as shown in Fig. 3. This is due to the two-band model in which the negative thermopower originated from $3d$ e_g electrons counterbalances effectively the positive thermopower created by O $2p$ holes. Consequently the total thermopower is suppressed by La-doping.

The electronic and magnetic properties in the La-doped compound ($x = 0.2$) change remarkably around 160 K. As for the thermopower, there is the onset of a steep drop at $T \cong 160$ K as shown in Fig. 3, in spite of the semiconductive behavior above 160 K. There is an anomaly in magnetic susceptibility and the onset temperature of this anomaly is also approximately 160 K (see Fig. 4c). In the Arrhenius relation of ρ and $1/T$ plotted in Fig. 5, there is also some transition around 160 K, implying that the conduction kinetic at low temperature is different from that at high temperature. The transitions in these properties around 160 K are likely to suggest a change in the electronic structure. One of the reasons for the rapid increase in the resistivity at $T < 160$ K may be the decreases in the densities of the mobile carriers.

The magnetic behavior of the La-doped compound is very similar to that in Pb-doped Bi-Sr-Co–O misfit layer compound (17). Then the results in Fig. 4c suggest that the La-doped compound involves antiferromagnetic interactions as well as Pb-doped Bi-Sr-Co–O compound. Since such an interaction restrains $3d$ electrons, they are localized more deeply and become less mobile at low temperature. The increase in the number of the less-mobile localized $3d$ electrons creates large negative thermopower (31) and counterbalances remarkably the positive thermopower due to the O $2p$ holes, resulting in the steep drop of the total thermopower at $T < 160$ K. The less mobile localized $3d$ electrons due to the antiferromagnetic interactions raise the energy levels of Co e_g parentages. Then the antiferromagnetic interactions assist in expanding the CT gaps.

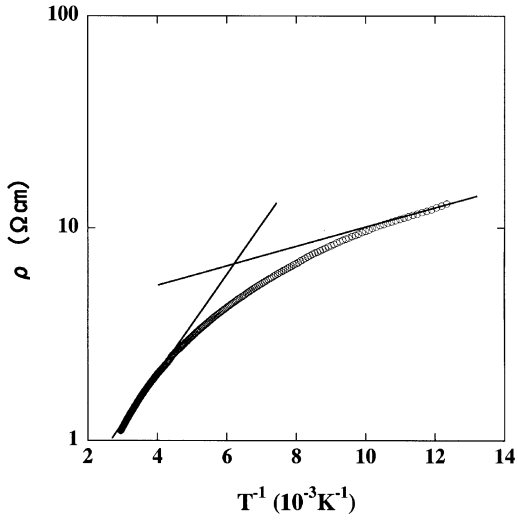

FIG. 5. Arrhenius plots of ρ and $1/T$ for the La-doped compound ($x = 0.2$).

5. SUMMARY

In order to understand the origin of low resistivity and high thermopower in the transition metal oxides with the lattice structure isomorphous to the 232-structure, the present study has prepared the compounds of $Bi_{1.5}Pb_{0.5}Ca_{2-x}M_xCo_2O_{8-\delta}$ by replacing M with Sc^{3+}, Y^{3+} or La^{3+} and also by employing $x = 0$, 0.1, 0.2 and 0.3. These procedures enable a smooth variation in the bond nature between Co and O ions in the crystal lattices through the changes in the lattice parameter, which promises significant knowledge as to the emergence of low resistivity and high thermopower. The XRD study indicates that the main lattice structure in these compounds is nearly isomorphous to $Bi_2Ca_3Co_2O_9$ (the 232-typed lattice), although there are satellite lines due to impurity phases but undetectably weak. As well as other 232-typed lattice such as $Bi_2Sr_3Co_2O_{9-\delta}$, the effective magnetic moment in $Bi_{1.5}Pb_{0.5}Ca_{2-x}M_xCo_2O_{8-\delta}$-system are larger in values than the expected ones. The mixed valences of Co ions due to the oxygen deficiency must be one of the reasons for the high effective magnetic moment.

As for the Sc- ($M = Sc^{3+}$) and Y-systems ($M = Y^{3+}$), the lattice parameter c decreases with x, and the resistivity decreases when x increases from 0 to 0.1, but increases with a further increase in x from 0.1 to 0.3. The thermopower in these compounds is large just like $Bi_{2-x}Pb_xSr_{3-y}Y_yCo_2O_{9-\delta}$. In every specimen, the Curie–Weiss law holds. The experimental value for the Curie constant estimates the effective magnetic moment which does not increase monotonously with x in both the systems. These behaviors are discussed in terms of the CT scheme with the effect of oxygen content.

In the La-doped compound ($x = 0.2$), the resistivity is very high, but there is a transition around 160 K in the electrical transport. The thermopower is in the same order as that in Sc- or Y-system, but there is a steep drop at $T <$ 160 K. This compound exhibits the magnetic behavior very different from that in Sc- or Y-system, although the Curie-Weiss law holds at $T > 200$ K, yielding a large effective magnetic moment. These phenomena are ascribed to the large ionic radius of La^{3+} which expands the CT gaps and results in antiferromagnetic interactions at low temperature. Though the two-band model holds in every system of the present study, the contribution of $3d$ e_g electrons is recognized most obviously in the steep drop of the thermopower in the La-doped compound at $T < 160$ K.

ACKNOWLEDGMENTS

The authors are very grateful for K. Yonekawa and D. Utsumi for their assistances on this study. This work was supported by a Grant-in-Aid for Science Research from Ministry of Education, Science and Culture, Japan (No.11650716), and by Takahashi Industrial and Economic Research Foundation. The SQUID magnetometer in the Ecotechnology System Laboratory, Yokohama National University, was used.

REFERENCES

1. G. D. Mahan, *Solid State Phys.* **51,** 81 (1998).
2. J. M. Ziman, "Principles of the Theory of Solids." Cambridge University Press, Cambridge, 1965.
3. T. Itoh, T. Kawata, T. Kitajima, and I. Terasaki, "Proceedings of the 17th International Conference On Thermoelectric (ICT'98) (Nagoya) p. 595." Institute of Electrical and Electronics Engineering, Picataway, NJ, 1998.
4. I. Terasaki, Y. Sasago, and K. Uchinokura, *Phys. Rev. B* **56,** R12,658 (1997).
5. R. Funahashi, I. Matsubara, H. Ikuta, T. Takeuchi, U. Mizutani, and S. Sodeoka, *Jpn. J. Appl. Phys.* **39,** L1127 (2000).
6. T. Yamamoto, I. Tsukada, K. Uchinokura, M. Takagi, T. Tsubone, M. Ichihara, and K. Kobayashi, *Jpn. J. Appl. Phys.* **39,** L747 (2000).
7. E. Iguchi, T. Itoga, H. Nakatugawa, F. Munakata, and K. Furuya, *J. Phys. D* **34,** 1017 (2001).
8. M. Abbate, J. C. Fuggle, A. Fujimori, L. H. Tjeng, C. T. Chen, R. Potze, G. A. Sawatzky, H.Eisaki, and S.Uchida, *Phys. Rev. B* **47,** 16124 (1993).
9. M. Abbate, R. Potze, G. A. Sawasky, and A. Fujimori, *Phys. Rev. B* **49,** 7210 (1994).
10. R. D. Shannon, *Acta Crystallogr. A* **32,** 751 (1976).
11. V. V. Vashuk, O. P. Ol'shevskaya, O. V. Strukova, and N. B. Nesterenko, *Inorg. Mater.* **33,** 398 (1997).
12. M. Hervieu, Ph. Boullay, C. Michel, A. Maignan, and B. Raveau, *J. Solid State Chem.* **142,** 305 (1999).
13. I. Tsukada, M. Nose, and K. Uchinokura, *J. Appl. Phys.*, **80,** 5691 (1996).
14. J. M. Tarascon, R. Ramcsh, P. Barboux, M. S. Hedge, and G. H. Hull, *Solid State Commun.* **71,** 663 (1989).
15. S. M. Laureiro, D. P. Young, and R. J. Cava, *Phys. Rev. B* **63,** 94109 (2000).
16. H. Nakatsugawa and E. Iguchi, *J. Phys.: Condens. Matter* **11,** 1711 (1999).
17. I. Tsukada, T. Yamamoto, M. Takagi, T. Tsubone, S. Konno, and K. Uchinokura, *J. Phys. Soc. Jpn.* **70,** 834 (2001).
18. I. Terasaki, T. Nakahashi, A. Maeda, and K. Uchinokura, *Phys. Rev. B* **47,** 451 (1993).
19. Y. Watanabe, D. C. Tsui, J. T. Birmingham, N. P. Ong, and J. M. Tarascon, *Phys. Rev. B* **43,** 3026 (1991).
20. J. M. Tarascon, Y. LePage, W. R. Mckinnon, R. Ramesh, M. Eibschutz, E. Tselepis, E. Wang, and G. W. Hull, *Physica, C* **167,** 20 (1990).
21. I. Tsukada, I. Terasaki, T. Hoshi, F. Yura, and K. Uchinokura, *J. Appl. Phys.* **76,** 13171 (1994).
22. T. Mizokawa, L. H. Tjeng, and P. G. Steeneken, *Phys. Rev. B* **64,** 115104 (2001).
23. H. Takahashi, F. Munakata, and M. Yamanaka *Phys. Rev. B* **53,** 3731 (1996).
24. P. M. Raccah and J. B. Goodenough, *Phys. Rev.* **155,** 935 (1967).
25. Y. LePage and W. R. McKinnon, *Phys. Rev. B* **40,** 6810 (1989).
26. M. C. MacDonald, "Thermoelectricity." Wiley, New York, 1962.
27. F. J. Blatt, "Physics of Electronic Conduction in Solids." McGraw-Hill, New York, 1968.
28. F. Munakata, K. Matsuura, K. Kubo, T. Kawano, and H. Yamauchi, *Phys. Rev. B* **45,** 10604 (1992).
29. M. Rubinstein, D. J. Gillespie, J. E. Snyder, and T. M. Tritt, *Phys. Rev. B* **56,** 5412 (1997).
30. H. Wakai, *J. Phys.: Condens. Matter.* **13,** 1627 (2001).
31. M. F. Mott and E. A. Davis, "Electronic Processes in Non-Crystalline Materials." Clarendon Press, Oxford, 1979.